

J. Interfacial Control of Deformation Twinning in Creep-Deformed TiAl/Ti₃Al Nanolaminate

Luke Hsiung

Chemistry and Materials Science Directorate

Lawrence Livermore National Laboratory

L-352, P.O. Box 808

Livermore, CA 9455-9900

(925) 424-3125; fax: (925) 424-3815; e-mail: hsiung1@llnl.gov

DOE Technology Development Area Specialist: Dr. Sidney Diamond

(202) 586-8032; fax: (202) 586-1600; e-mail: sid.diamond@ee.doe.gov

ORNL Technical Advisor: D. Ray Johnson

(805) 576-6832; fax: (865) 574-6098; e-mail: johnsondr@ornl.gov

Contractor: Oak Ridge National Laboratory, Oak Ridge, Tennessee

Prime Contract No: DE-AC05-00OR22725

Subcontractor: Lawrence Livermore National Laboratory, Livermore, California

Objectives

- Exploit thermomechanical-processing techniques to fabricate TiAl/Ti₃Al nanolaminate composites at sizes from lamella width down to nanometer-length-scales.
- Characterize the microstructure and elevated-temperature creep resistance of the nanolaminate composites.
- Investigate the fundamental relationships among microstructures, alloying additions, and mechanical properties of the nanolaminate composites to achieve the desired properties of the composites for high-temperature structural applications.

Approach

- Employ in-situ laminate composites with nominal compositions of Ti-47Al-2Cr-2Nb, Ti-46Al-3Nb-1W-0.1B, and Ti-46Al-3Nb-2W-0.1B (at. %).
- Conduct creep tests in a dead-load creep machine with a lever arm ratio of 16:1. Tests were performed in air in a split furnace with three zones at 760 and 815°C.
- Examine the microstructures of creep-deformed samples using a JEOL-200CX transmission electron microscope (TEM).

Accomplishments

- Collaborated with Oak Ridge National Laboratory (ORNL) (C.T. Liu) to fabricate TiAl/Ti₃Al laminate composites with high tungsten content using hot-extrusion processing techniques.
- Characterized and measured the effect of tungsten addition on creep resistance of the TiAl/Ti₃Al laminate composites.

Future Direction

- Continue to collaborate with ORNL to fabricate an oxidation- and heat-resistant class of TiAl/Ti₃Al laminate composites with high niobium content (>10 at %) using the hot-extrusion processes.

- Continue to investigate the effects of alloying additions and deformation (mechanical) twinning on the microstructural stability and creep resistance of the nanolaminate composites at elevated temperatures of up to 850°C.

Introduction

One of the unique deformation substructures of TiAl/Ti₃Al laminate composite is the formation of deformation twins (DTs) within γ lamellae. The twinning phenomena have been found to be significantly promoted within ultrafine lamellar TiAl as a result of refined lamellar spacing presumably because the increment of lamellar interfaces provides even more nucleation sites for twinning. Although it has been well known that deformation twinning can be activated by the homogeneous glide of $1/6\langle 11\bar{2} \rangle$ twinning dislocations on the $\{111\}$ planes, the underlying twinning mechanism still remains unclear. To better design lamellar alloys for high-temperature applications, it is important to understand and gain insights regarding the role of lamellar interfaces in the twinning process, as well as the mechanical behavior of the alloys. Accordingly, this investigation was conducted to elucidate the deformation twinning mechanisms in TiAl/Ti₃Al nanolaminate.

Approach

A TiAl/Ti₃Al nanolaminate composite was fabricated at ORNL by a hot extrusion process, which involves hot-extrusion of a cast TiAl alloy at 1350°C. After extrusion, the alloy was stress-relieved at 900°C in a vacuum ($\sim 10^{-4}$ Pa) for 2 h. Creep tests were conducted in a dead-load creep machine with a lever arm ratio of 16:1. For the current study, the deformation substructures of the specimen were investigated [tested at 760°C, 138 MPa (creep strain: 0.25%); 760°C, 518 MPa (creep strain: 3.6%); and 815°C, 420 MPa (creep strain: 1.7%)]. TEM foils were prepared by twinjet electropolishing in a solution of 60 vol % methanol, 35 vol % butyl alcohol, and 5 vol % perchloric acid at ~ 15 V and -30°C . The microstructures of the tested samples were examined using a JEOL-200CX TEM equipped with a double-tilt goniometer stage. Images of dislocations were mostly recorded using weak-beam dark field (WBDF) imaging techniques under $g(3g)$ two-beam diffraction conditions with the deviation factor $\omega (= \xi_g s) > \sim 1$, where ξ_g is the extinction distance and s is the deviation distance from the exact Bragg position. The $g \bullet b$ invisibility

criteria used for determining the Burgers vector of Shockley partials are described as follows:¹ (a) invisible if $g \bullet b = 0$ or $\pm 1/3$; (b) invisible if $g \bullet b = -2/3$ but visible if $g \bullet b = +2/3$ provided the deviation factor $\omega > \sim 1$; (c) invisible if $g \bullet b = +4/3$ but visible if $g \bullet b = -4/3$ provided the deviation factor $\omega > \sim 1$.

Results

Microstructure

Figure 1 is a bright-field TEM image showing a typical edge-on microstructure within a TiAl (γ)-Ti₃Al (α_2) nanolaminate. In general, the material contains two types of interfaces:²

1. The γ/α_2 interphase interface, which has a usual orientation relationship $(0001)_{\alpha_2} \parallel (111)_\gamma$ and $\langle 11\bar{2}0 \rangle_{\alpha_2} \parallel \langle 1\bar{1}0 \rangle_\gamma$.
2. The γ/γ twin-related interface, which includes true-twin (180° rotational) and pseudo-twin (60° and/or 120° rotational) interfaces.

Here, the width of the α_2 layers ranges from 10 to 50 nm, and the width of the γ layers ranges from 150 to 300 nm. Figure 2 is a WBDF TEM image showing a typical dislocation substructure within the nanolaminate. Both lattice dislocations (LDs) within the γ layer and a high density of interfacial dislocations (IDs) on inclined interfaces can be clearly seen. The density of the IDs is much greater than that of the LDs, and the LDs are primarily threading dislocations, which terminate their two ends at the interfaces. While the IDs on semi-coherent γ/α_2 and γ/γ pseudo-twin interfaces are $1/6\langle 112 \rangle$ or $1/3\langle 112 \rangle$ type misfit dislocations,³ those on the γ/γ true-twin interface are mainly $1/6[11\bar{2}]$ type twinning dislocations or geometry necessary dislocations for accommodating the departure of the true-twin interface from the exact (111) twin plane.

Deformation Twinning and Proposed Mechanisms

When the nanolaminate was creep-deformed at 760°C and 518 MPa, a deformation substructure

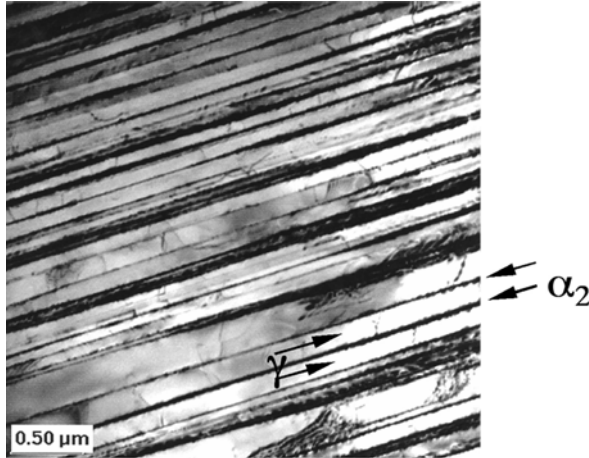


Figure 1. Bright-field TEM image showing a lamellar grain from an edge-on orientation.

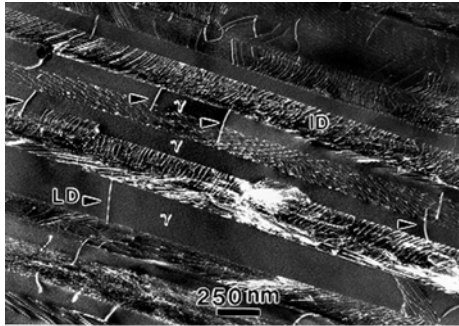
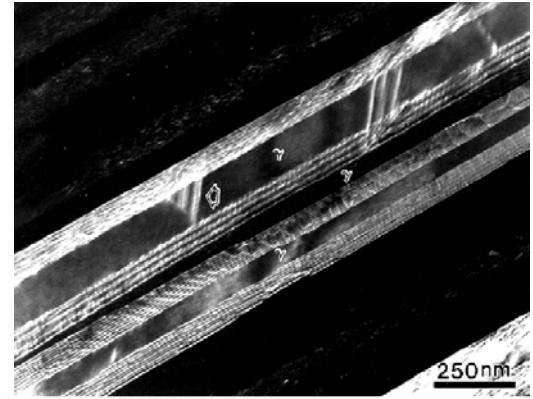
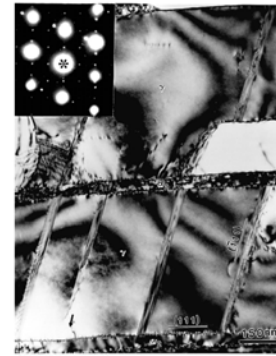


Figure 2. Weak-beam dark-field TEM image showing a typical dislocation structure of TiAl nanolaminate.

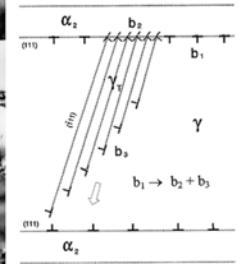
associated with DTs within γ layers was developed. Typical examples of the formation of $(\bar{1}11)$ -type DTs within the nanolaminate are shown in Figures 3 (a) and (b). Note that one of the twin lamellae was still growing between two lamellar interfaces, and its growth would be eventually blocked by the lower interface. This observation suggests that the interfaces are preferred nucleation sites for DTs, presumably resulting from the high local stresses caused by the pileup of interface dislocations. Accordingly, it is proposed that deformation twinning in the TiAl-Ti₃Al nanolaminate can be viewed as a stress relaxation process to relieve the local stress concentration caused by the pile-up of interfacial dislocations during deformation. The effective stress (τ_e) at the tip of the pile-up of n dislocations can be evaluated by $\tau_e = n\tau_i$ [4], where τ_i is the resolved shear stress acting on the interface. To relieve the stress concentration, deformation twinning in γ layers is therefore taking place by a dislocation reaction



(a)



(b)



(c)

Figure 3. Dark-field (a) and bright-field (b) TEM images showing several $(\bar{1}11)$ type deformation twins formed a growing process toward another interface. Schematic illustration (c) of the nucleation of a $(\bar{1}11)$ type DT from a γ/α_2 interface, where b_1 , b_2 , and b_3 denote the interfacial, stair-rod, and twinning dislocations, respectively.

based upon a stair-rod cross-slip mechanism.^{5,6} As for an example of the $(\bar{1}11)$ -type DTs formed in the nanolaminate, the corresponding dislocation reaction (dissociation) is proposed to be $1/6[\bar{1}2\bar{1}]_{(111)} \rightarrow 1/6[011]_{(100)} + 1/6[\bar{1}1\bar{2}]_{(\bar{1}11)}$. The $(\bar{1}11)$ -type DT is accordingly formed by a successive cross-slip of the twinning dislocations $1/6[\bar{1}1\bar{2}]$ on the $(\bar{1}11)$ plane, leaving the stair-rod dislocations $1/6[011]$ on the (100) plane. Twin (stacking) faults are subsequently formed on the interfaces between the γ layer and the DTs. This is schematically illustrated in Figure 3 (c).

The formation of stair-rod dislocations at the intersections between the DTs and the α_2 layer is evi-

denced in Figure 4, where the array of $1/6[011]$ stair-rod dislocations become invisible [Figure 4(a)] or visible [Figure 4(b)] when a reflection vector (g) 200 or 021 is used for imaging. It is noted that the individual stair-rod dislocation is not resolvable because of a narrow distance (0.25 nm) between two stair-rod dislocations. The significance of the proposed mechanism is to reveal that there are several barriers to be overcome in order to activate the twinning reaction. These barriers include (1) the repulsive force (F) between the interfacial (Shockley) and stair-rod dislocations, (2) the increase of line energy due to the dislocation dissociation, and (3) the increase of interfacial energy due to the formation of twin faults. Among them the repulsive force (F) between the interfacial (Shockley) and stair-rod dislocations is considered to be rate-controlling. That is, a critical (minimum) stress (τ_c) is required to activate the dissociation reaction for twinning.

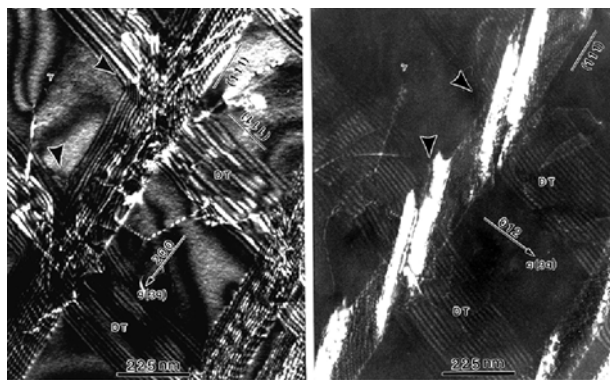


Figure 4. Paired WBDF images demonstrating the existence of the array of $1/6[011]$ stair-rod dislocations at the intersections (indicated by arrows) between the $(\bar{1}11)$ -type DT and α_2 layer: (a) Invisible at $g = 200$ ($g \cdot b = 0$), (b) visible at $g = 021$, Z (zone axis) $\approx [0\bar{1}2]$.

Conclusion

The role of interfaces in deformation twinning of $TiAl/Ti_3Al$ nanolaminate has been investigated. Since the multiplication of lattice dislocations within both γ and α_2 lamellae becomes very limited at a low stress level, the motion of interfacial dislocations (i.e., interface sliding) becomes an important deformation mode. Impinged lattice dislocations were observed to impede the movement of interfacial dislocations, which move in a cooperative fashion along the lamellar interfaces. The impediment of dislocation motion subsequently causes a dislocation

pile-up in front of the obstacle as creep strain accumulates. When the laminate deforms at a high stress level, deformation twinning becomes a predominant deformation mode. The deformation twinning is suggested to be a stress relaxation process for the concentration of stress at the head of each dislocation pile-up. An interface-controlled twinning mechanism based upon a stair-rod cross-slip dislocation reaction is proposed and verified.

References

1. J. W. Edington, *Practical Electron Microscopy in Materials Science*, Van Nostrand Reinhold, New York, 1976.
2. M. Yamaguchi and Y. Umakoshi, *Progress in Materials Science* **34**, 1 (1990).
3. L. M. Hsiung and T.G. Nieh, *Mater. Sci. & Eng.* **A239–240**, 438 (1997).
4. J. D. Eshelby, F. C. Frank and F. R. N. Nabarro, *Phil. Mag.* **42**, 351 (1951).
5. Fujita and T. Mori, *Scripta Metall.* **9**, 631 (1975).
6. T. Mori and H. Fujita, *Acta Metall.* **28**, 771 (1980).

Publications/Presentations

1. L. Hsiung, "Interface Sliding and Migration in an Ultrafine Lamellar Structure," invited keynote presentation to the International Conference on Computational and Experimental Engineering & Sciences, Madeira, Portugal, July 28, 2004.
2. Andrea M. Hodge, L. Hsiung, T. G. Nieh, "Creep of Nearly Lamellar $TiAl$ Alloys Containing 1.0 and 2.0 at % W," presented at Materials Science and Technology 2004, September 27, 2004.
3. L. M. Hsiung, T.G. Nieh, "Microstructures and Properties of Powder Metallurgy $TiAl$ Alloys," *Mater. Sci. & Eng.* **A364**, 1 (2004).
4. A. Hodge, L. M. Hsiung, T. G. Nieh, "Creep of Nearly Lamellar $TiAl$ Alloy Containing W," *Scripta Mater.* **51**, 411 (2004).
5. Luke L. Hsiung and Clyde L. Briant, *Segregation of Tungsten to Interfaces in Lamellar $TiAl$* , Lawrence Livermore National Laboratory, April 6, 2004.
6. Luke L. Hsiung and Andrea M. Hodge, *Effects of W on Creep Deformation of Nearly Lamellar $TiAl$* , Lawrence Livermore National Laboratory, July 16, 2004.